



# Applications of bivariate generalized Pareto distribution and the threshold choice

Toshikazu Kitano  
Nagoya Institute of Technology

# One of the biggest disasters in Japan, 2018

## Typhoon Jebi causes record storm surge of over 3 meters in Osaka

September 5, 2018 (Mainichi Japan)

Japanese



A storm surge caused by Typhoon Jebi floods over a wharf as containers are washed out to sea at Rokko Island in Kobe's Higashinada Ward, in western Japan, on Sept. 4, 2018. (Mainichi)

Powerful Typhoon Jebi triggered a historic storm surge of 3.29 meters in Osaka Prefecture in western Japan on Sept. 4, surpassing the previous high of 2.93 meters recorded in 1961 due to Typhoon Nancy, which killed 194 people.



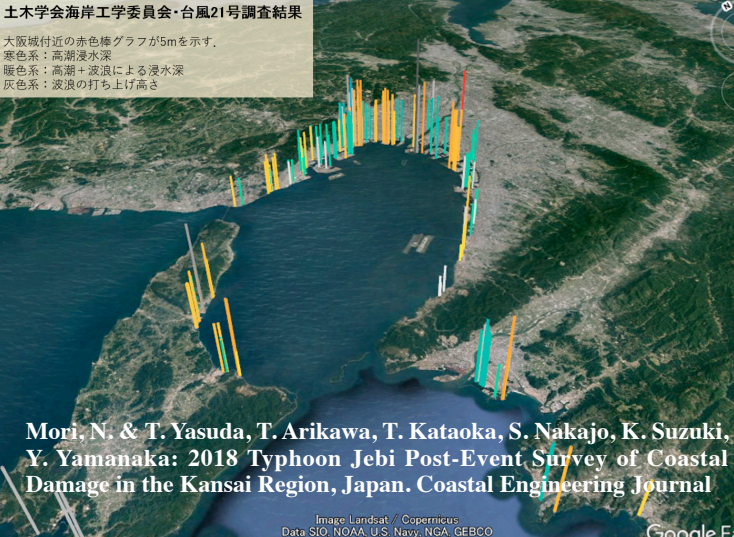
Kansai International Airport is flooded in a storm surge on Sept. 4, 2018. (Asahi Shimibun file photo)



A damaged tanker is seen after colliding into the bridge connecting Kansai International Airport to mainland Osaka Prefecture due to strong winds from Typhoon Jebi on Sept. 4, 2018. (Mainichi)



大阪城付近の赤色棒グラフが5mを示す。  
寒色系：高潮浸水深  
暖色系：高潮+波浪による浸水深  
灰色系：波浪の打ち上げ高さ



Kansai International Airport is flooded in a storm surge on Sept. 4, 2018. (Asahi Shimbun file photo)

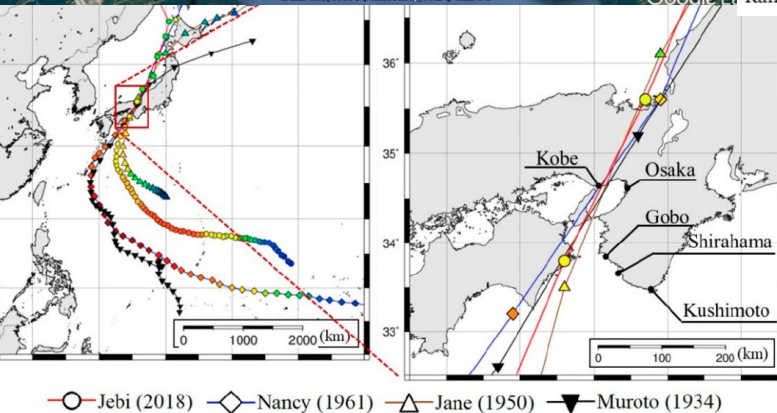
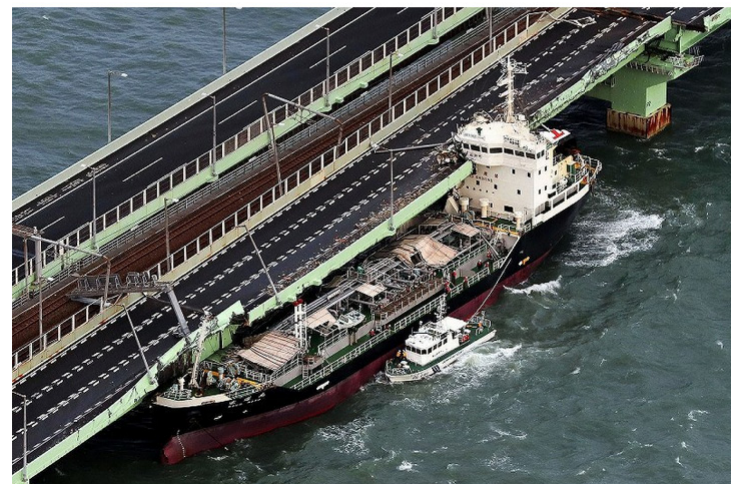


Figure 1. Most notable storm tracks to affect Osaka Bay area. Best track data for Jebi and Nancy from Japan Meteorological Agency (JMA) [1,2], while Jane and Muroto's are from NOAA's IBT database [3]. Note that there is no pressure information for Muroto's track data.



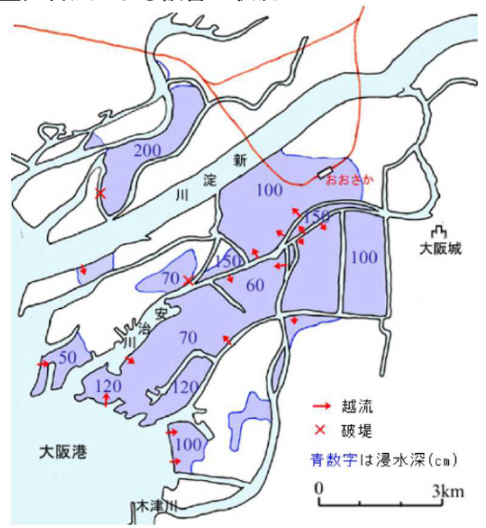
A damaged tanker is seen after colliding into the bridge connecting Kansai International Airport to mainland Osaka Prefecture due to strong winds from Typhoon Jebi on Sept. 4, 2018. (Mainichi)

**Field Survey of 2018 Typhoon Jebi in Japan: Lessons for Disaster Risk Management**, by Takabatake, T. et al., Geoscience, 2018.

# 第2室戸台風と平成30年台風21号

○大阪湾では、これまで主に第2室戸台風により最高潮位を記録。(第2室戸台風:大阪府下で被災者約26万人におよぶ被害)  
○台風21号では管内の太平洋側の8潮位観測所のうち、5地点で記録を更新。

## ・第2室戸台風による被害の状況

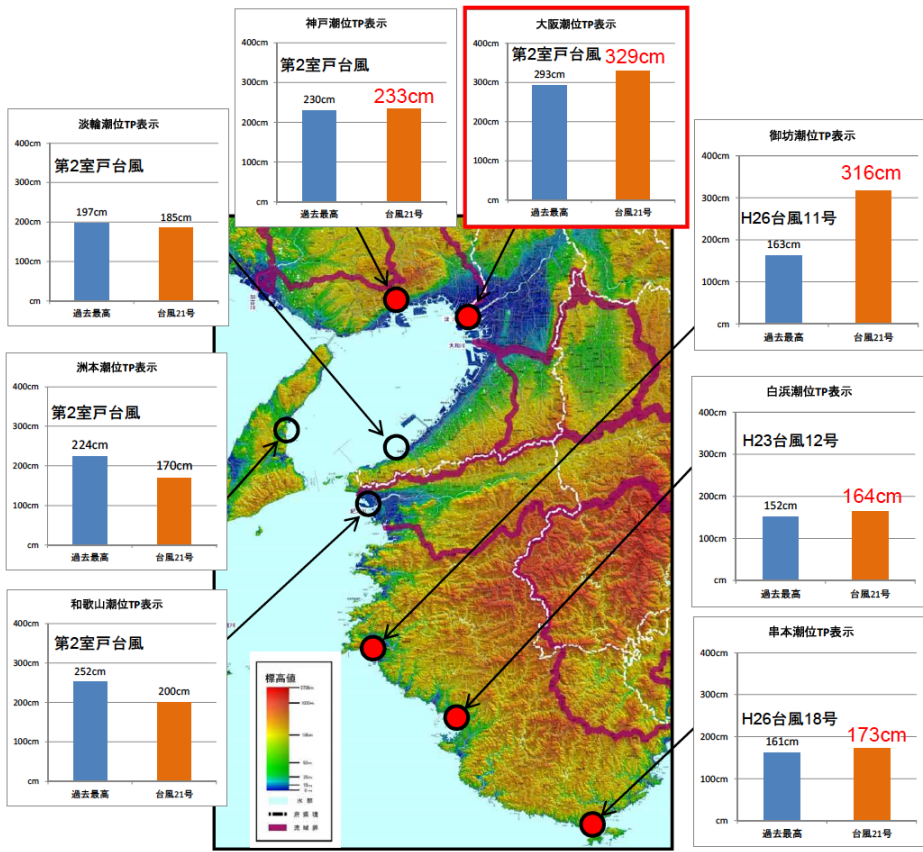


引用:大阪管区気象台(1962):第2室戸台風報告。大阪管区異常気象調査報告9.3

・大阪府下の浸水被害(大阪府HP):  
床上約61,000戸、床下約60,000戸、  
被災者約26万人、死者32人



## ・平成30年台風21号の潮位と過去最高潮位との比較





○台風21号において、大阪湾ではこれまでの最高潮位TP+293cm(第2室戸台風1961(S36).9.16)を超過し、潮位TP+329cm(9/4 14:18)を記録。

・第2室戸台風(昭和36年9月)の高潮による大阪市内での大規模な浸水被害を契機に高潮対策を実施。

三大水門(S45完成)、毛馬排水機場(S58改築)、淀川大堰(S58完成)、大阪湾岸及び淀川の高潮堤(S44完成)、淀川陸間(S46完成)等

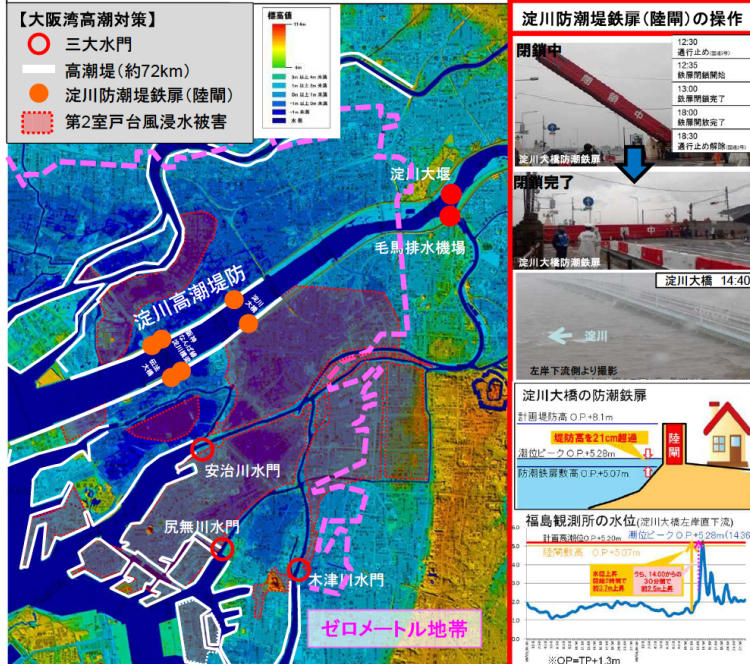
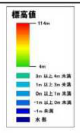
○上記、大阪湾高潮対策や、淀川防潮堤鉄扉(陸間)・大阪府三大水門等の適切な操作により、大阪市街地の高潮による浸水被害を回避。

・淀川防潮堤鉄扉(陸間)6箇所※(R2淀川大橋、R43伝法大橋、阪神なんば線淀川橋梁)の閉鎖(9/4 13:30)、大阪府三大水門の閉門(9/4 13:43)等を実施。

(※淀川防潮堤鉄扉(陸間)6箇所の閉鎖は、1979年(昭和54年)9月以来の39年ぶり。)

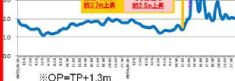
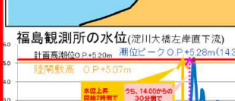
## 【大阪湾高潮対策】

- 三大水門
- 高潮堤(約72km)
- 淀川防潮堤鉄扉(陸間)
- 第2室戸台風浸水被害



## 淀川防潮堤鉄扉(陸間)の操作

閉鎖中	12:30
	通行止め(両側)
	12:35
	鉄扉閉鎖開始
	13:00
	鉄扉閉鎖完了
	19:00
	鉄扉開放完了
	19:30
	通行止め解除(両側)



## 淀川大堰、毛馬排水機場、大阪府三大水門の操作



＜大阪府三大水門川水門と毛馬排水機場の稼働実績＞  
 ①三大水門高潮警報発令(9/4 6:30) → ②三大水門 閉 操作完了(9/4 13:43) →  
 ③毛馬排水機場 運転 開始(9/4 13:45) → ④木津川水門 開 操作完了(9/4 18:36) →  
 ⑤安治川水門 開 操作完了(9/4 18:49) → ⑥毛馬排水機場 運転 停止(9/4 19:55) →  
 ⑦尻無川水門 開 操作完了(9/4 21:07)

台風21号による高潮は、第二室戸台風(昭和36年)を越える規模(ほぼ同程度)  
 淀川での高潮の河川遡上、高潮による水位が堤防高を超過。大阪府の3大水門の閉鎖による浸水回避。  
 淀川本川の3橋の防潮鉄扉(陸間)の閉鎖(1979年以来)

- \* Large area innandated
- \* Yodo River also damaged
- \* Ship landed (like 2011)



■ 伊勢湾台風による浸水状況図

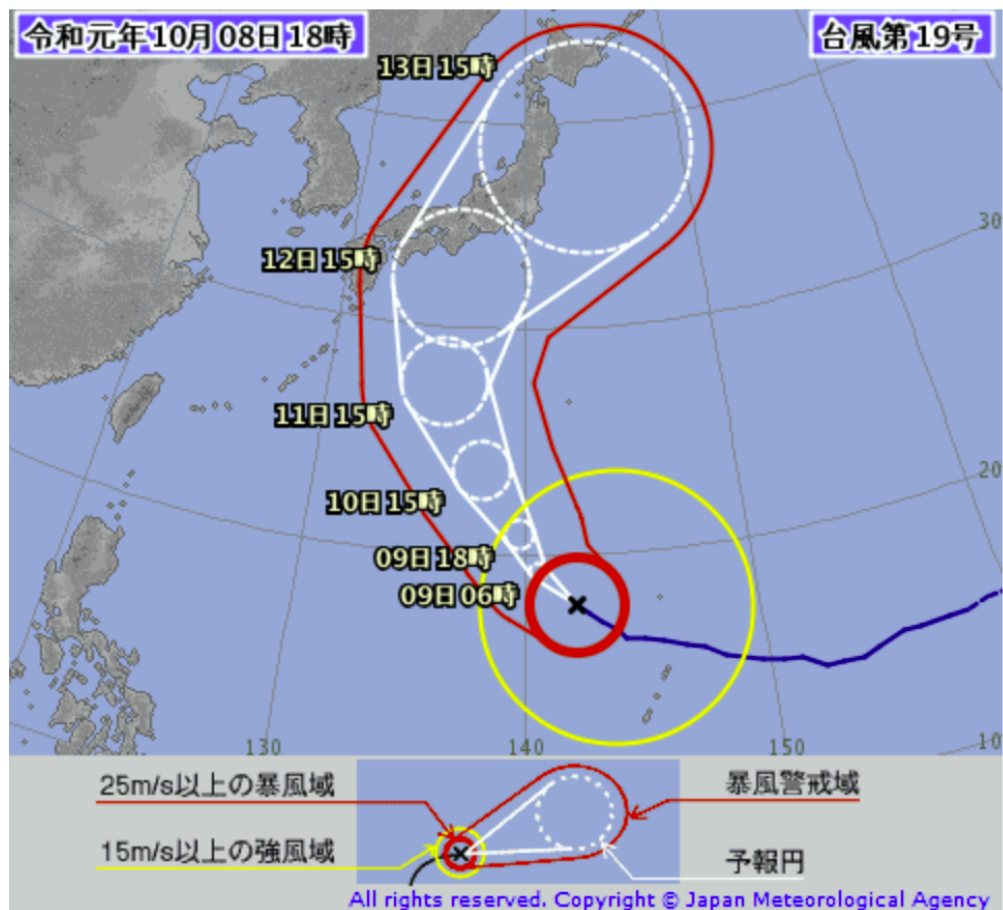


■ 伊勢湾台風および13号台風(昭和28年)の経路図

1959, September 26th  
Isewan Typhoon

京都大学名誉教授  
岩垣 雄一 撮影  
京都大学防災研究所教授  
間瀬 肇 整理





非表示

## 台風第19号 (ハギビス)

令和元年10月08日18時45分 発表

### <08日18時の実況>

大きさ	大型
強さ	猛烈な
存在地域	マリアナ諸島
中心位置	北緯 18度00分(18.0度)
	東経 142度10分(142.2度)
進行方向、速さ	北西 20km/h(12kt)
中心気圧	915hPa
中心付近の最大風速	55m/s(105kt)
最大瞬間風速	75m/s(150kt)
25m/s以上の暴風域	全域 220km(120NM)
15m/s以上の強風域	東側 800km(425NM)
	西側 440km(240NM)

### <09日06時の予報>

強さ	猛烈な
----	-----

## 千葉まだ19万戸停電 断水も



KYODO, JIJI, STAFF REPORT

As of 7 p.m. Friday, some 185,000 households were still without electricity, down from the peak of 935,000 logged on Monday and 280,000 late Thursday, according to Tokyo Electric officials.

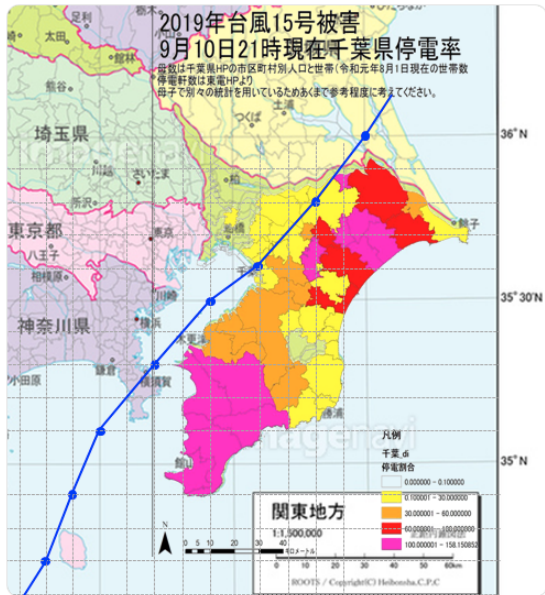
菊地 章(気象予報士)

@AkirAK54

[フォローする](#)

千葉県被災地の皆様には心よりお見舞い申し上げます。停電地域と台風経路の関係図が見つからないので作ってみました。台風の進行方向右側が危険半円であることが顕著に見られます。

- ・ 停電地域 10日21時状況（東電HP）  
・ 中心位置 9日0～7時（デジタル台風HP）

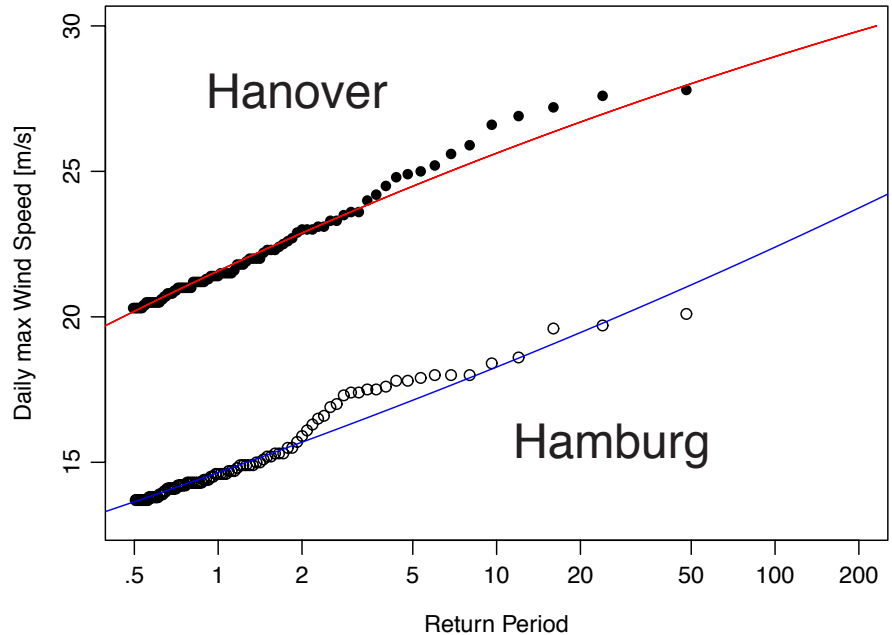


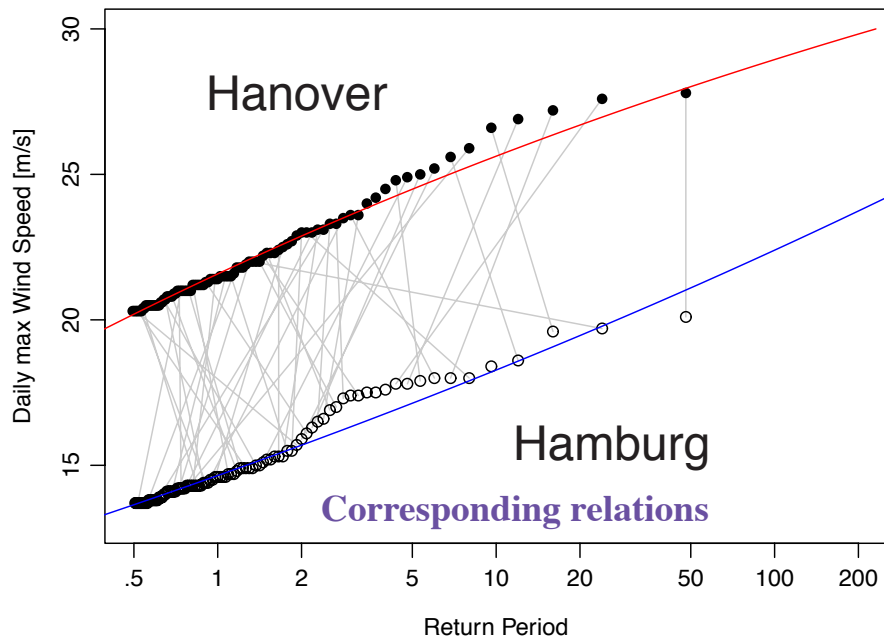
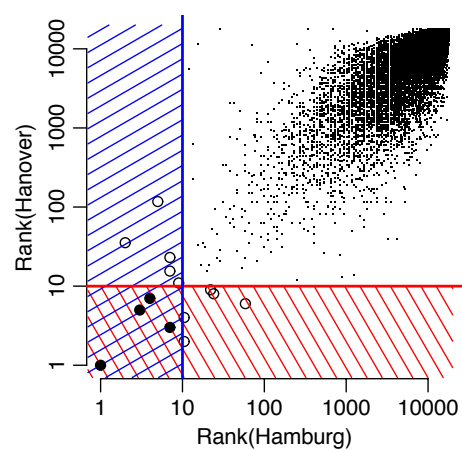
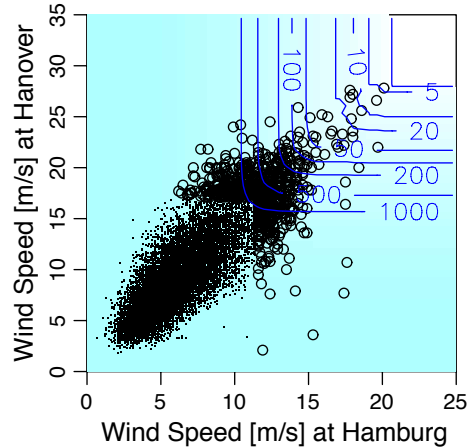
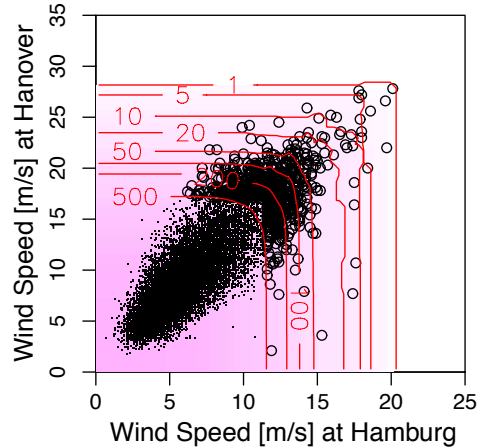


# Dependency of Extremes

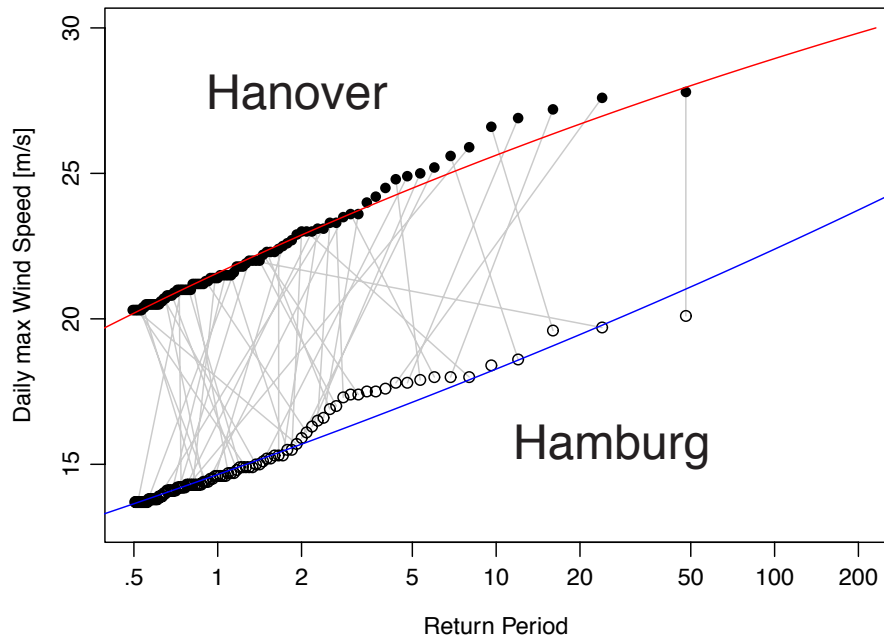
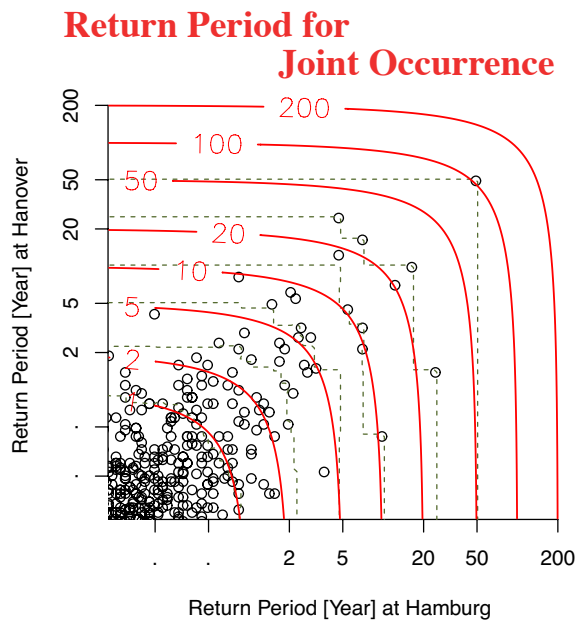
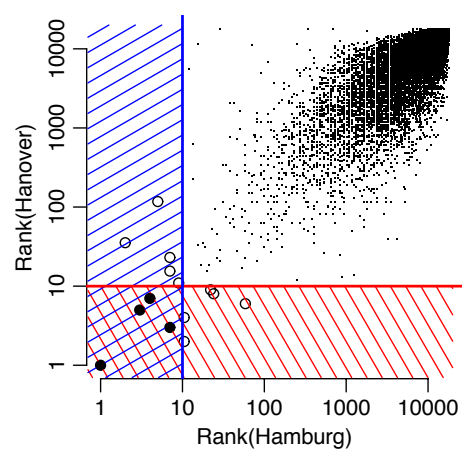
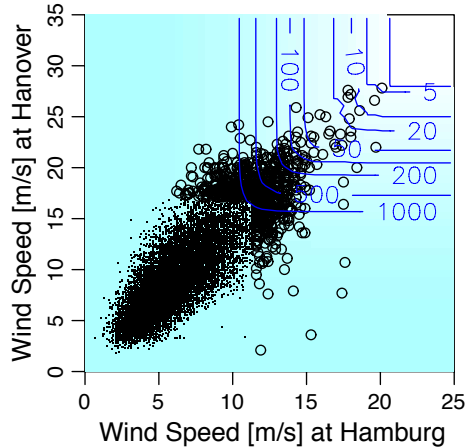
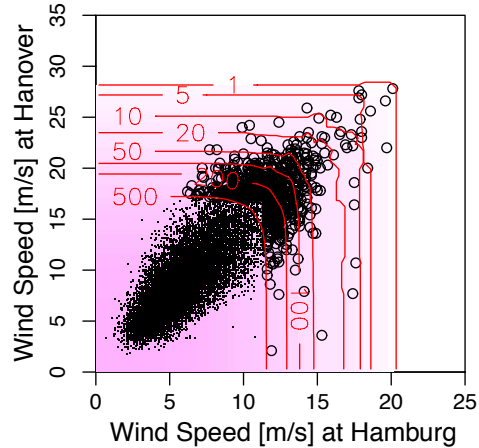
When spatially near communities are attacked at the **same time**, disaster will expand more.

Support, Back-up & Recovery will become more difficult than ...



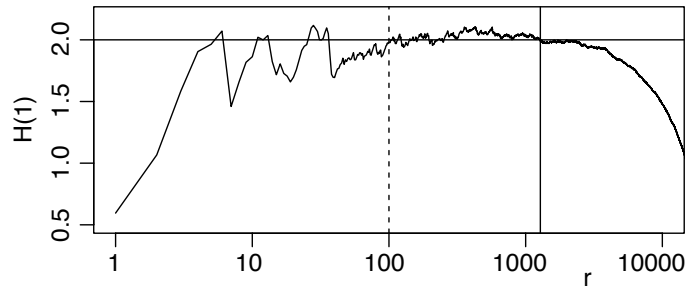






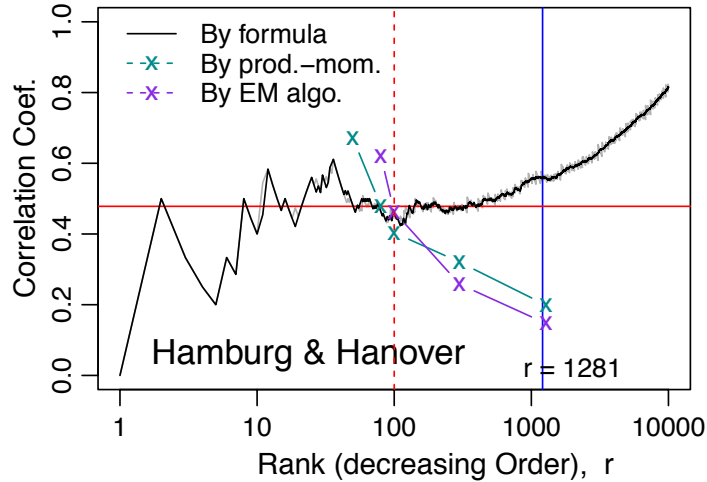
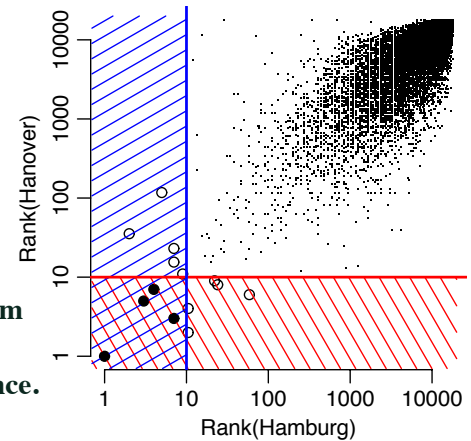
# Extremes by POT requires a threshold. (Peaks Over Threshold)

## Thresh. Choice by the conventional method

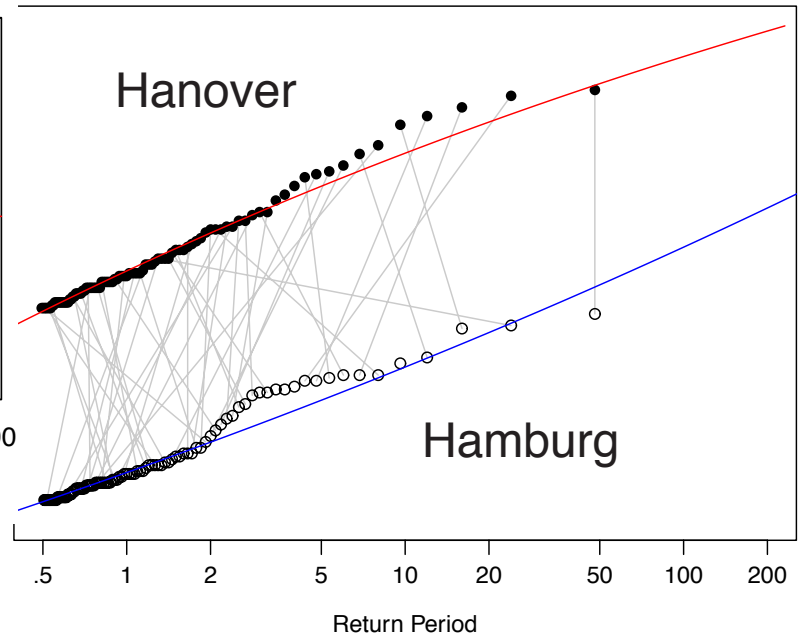


Thresh. Choice should be determined by the correlations, because the dependence problem can be solved by the properties of dependence.

**It is a logic.**



## Thresh. Choice by the method of correlation coefficient of occurrence numbers







<http://www.jamstec.go.jp/tougou/program/index.html>

## Integrated Research Program for Advancing Climate Models



MEXT

MINISTRY OF EDUCATION,  
CULTURE, SPORTS,  
SCIENCE AND TECHNOLOGY-JAPAN

This program aims to further develop climate models and to reflect the knowledge gained through them in the adaptation plans of actual regions in coordination with socioeconomic scenarios.

Area Theme A

**Prediction and Projection of  
Large-Scale Climate  
Changes Based on  
Advanced Model  
Development**

[READ MORE >](#)

Area Theme B

**Sophisticated Earth system  
model for evaluating  
emission reductions needed**

[READ MORE >](#)

MRI-NHRCM  
NHRCM Area Theme C

527x804x50

**Integrated Climate Change  
Projection**

[READ MORE >](#)

Area Theme D

**Integrated Hazard  
Prediction**

[READ MORE >](#)

How will global warming affect typhoons, floods, sediment disasters, and river flows? Theme D aims to project how devastating these disasters will change over the next 100 years and scientifically reveals the relationship between global warming and disasters. Mainly the following two analysis methods will be adopted: the first one is to quantify the probability of climate change impact on typhoons and flooding etc. and the second one is to assess the impact of climate change with the worst case scenarios that consider extraordinary situations such as super typhoons. In recent years, Japan as well as other countries have been affected by frequent and unprecedented disasters. Potential damages by such record-breaking disasters enhanced by climate change should be assessed from scientific and engineering perspectives. Moreover, we hope to provide basic information on appropriate measures needed in the future by understanding also the economic impacts.

## Projecting the impact of global warming on disasters and elucidating the trend in future with no-regret adaptation strategies.

Area Representative : **Eiichi Nakakita** (Professor, Disaster Prevention Research Institute, Kyoto University)

**To evaluate the uncertainty requires the extreme value theory and the statistical techniques to the applications.**

Subject	Representative
(i) Long-term assessment of intensity and frequency of extreme hazards	Nobuhito Mori Disaster Prevention Research Institute, Kyoto University, Associate Professor
(ii) Seamless hazard prediction until the end of the 21st century	Kenji Tanaka Disaster Prevention Research Institute, Kyoto University, Associate Professor
(iii) Hazard analysis of past disasters and assessment of climate change factors	Tetsuya Takemi Disaster Prevention Research Institute, Kyoto University, Associate Professor
(iv) Hazard assessment in Asian and Pacific countries and international cooperation	Yasuto Tachikawa Graduate School of Engineering, Kyoto University, Professor
(v) No-regret adaptation strategies with consideration for various changes	Hirokazu Tatano Disaster Prevention Research Institute, Kyoto University, Professor
(vi) <u>Development of bias correction methods and extreme values assessment technology</u>	<u>Toshikazu Kitano</u> Department of Civil Engineering, Nagoya Institute of Technology, Professor

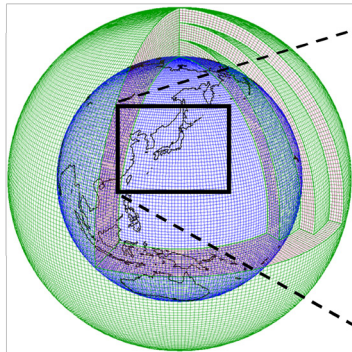
Area Theme D

**Integrated Hazard  
Prediction**

READ MORE >

## AGCM

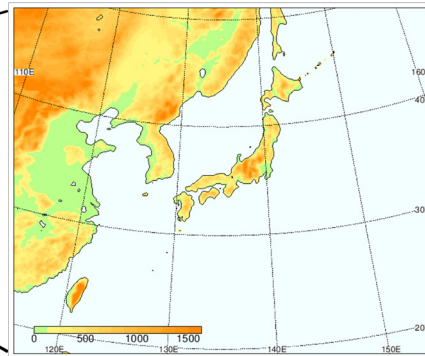
(水平解像度約60km)



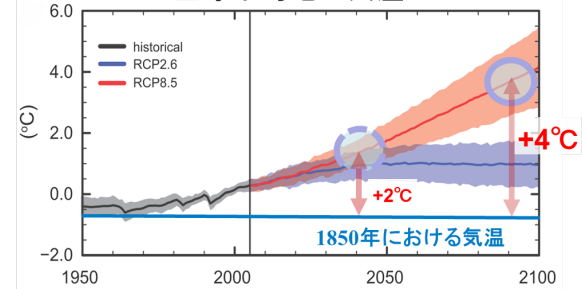
(画像:気象庁提供)

## NHRCM

(水平格子間隔20km)



## 全球平均地上気温



0km AGCM

100メンバ

非温暖化100メンバ

90メンバ

(6ΔT × 15δT)

本域 20km

50メンバ

90メンバ

メウスケール

1951

過去実験

2010

将来実験

60年

Welcome to d4PDF

Planning for adaptation to global warming will be based on impact assessments of disasters, agriculture, water resources, ecosystems, human health, and so on, in each region. For each impact assessment, detailed projections of extreme events such as heavy rainfall, heat wave, drought, and strong wind are required at the regional scale as well as projections of climatological temperature and precipitation. An unprecedentedly large ensemble of climate simulations with a 60 km atmospheric general circulation model and dynamical downscaling with a 20 km regional climate model have been performed to obtain probabilistic future projections of low-frequency local-scale events. The simulation outputs are open to the public as a database called "Database for Policy Decision-Making for Future Climate Change" (d4PDF), which is intended to be utilized for impact assessment studies and adaptation planning for global warming.



The importance of **bivariate extreme statistics**:

Overlap of several hazards: storm surge, high waves, river runoff and flooding etc. **accumulates risk** and its prediction will become troublesome.

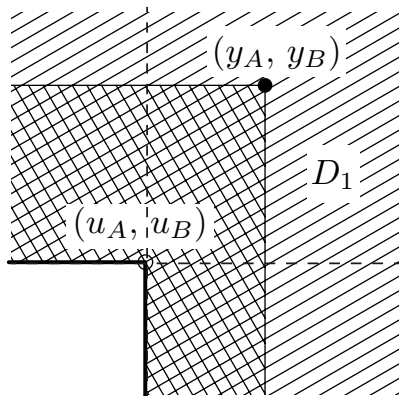
Simultaneous occurrences (or **joint occurrences**) at several sites (at least two important sites) also aggregate the loss by damage, and they will enlarge the loss **more than the proportional one**.

The importance of statistical distribution of bivariate extremes is now increasing in disaster risk reduction plan, but the **bivariate GP distribution** has been **not yet developed enough** for those applications.

One of the reasons is the **unclearness of mathematical understanding** of the multivariate (**bivariate**) extremes for the practical engineers.

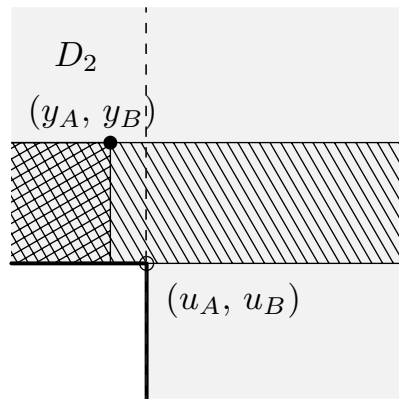
Here let us give a glance  
to the probability distribution:

$$F_u = \frac{\lambda_*(y_A \wedge u_A, y_B \wedge u_B) - \lambda_*(y_A, y_B)}{\lambda_*(u_A, u_B)}$$



case 1

$$\bar{F}_u(y_A, y_B) = 1 - F_u(y_A, y_B) = \frac{\lambda_*(y_A, y_B)}{\lambda_*(u_A, u_B)}$$



case 2

$$F_u(y_A, y_B) = \frac{\lambda_B(u_B) - \lambda_B(y_B) - \{\lambda_{AB}(y_A, u_B) - \lambda_{AB}(y_A, y_B)\}}{\lambda_*(u_A, u_B)}$$

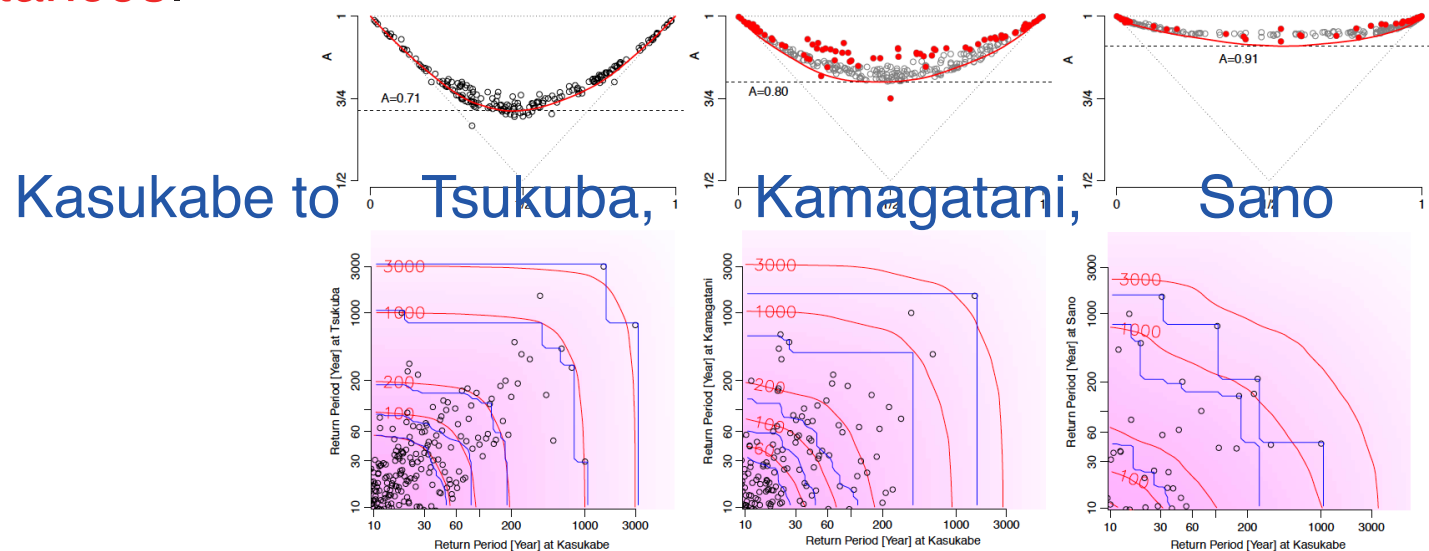
where we make the function  $\lambda_*$  **endlessly**, ...

One of the simplest ones is:

$$\lambda_*(y_A, y_B) = \left\{ \lambda_A^{1/\alpha}(y_A) + \lambda_B^{1/\alpha}(y_B) \right\}^\alpha$$

And therefore, though GP distribution **requires a suitable threshold** to extract the extremes of hazard magnitudes, the methods of **threshold choice** have not been enough discussed for bivariate extremes. This research focuses on the **correlation coefficient of occurrence rates**, whose efficiency is examined through the observed data of wind velocities at **two cities**.

And the numerous datasets of **daily rainfall in d4PDF** are also **applied** to **nonparametric analysis of bivariate extremes** to demonstrate the spacial **change of dependence of the pairwise points against the distances**.



dependent <---

---> independent



Fig.1 shows the two types of occurrence numbers for bivariate extremes. When a threshold  $u_A$  (or  $u_B$ ) is given for each component, we can count the excess number  $k_A$  (or  $k_B$ ) of extremes  $Y_A$  (or  $Y_B$ ) for the threshold, as

$$k_A(u_A) = \sum_{i=1}^n \mathbf{1}\{Y_A(i) > u_A\}, \quad k_B(u_B) = \sum_{i=1}^n \mathbf{1}\{Y_B(i) > u_B\} \quad (1)$$

where  $\mathbf{1}\{\text{condition}\}$  stands for 1 or 0 as the condition is true or false, respectively, and  $i$  is an indicator to check all data whose sample size is  $n$ . The joint occurrence number  $k_{AB}$  is defined as the excess number against both

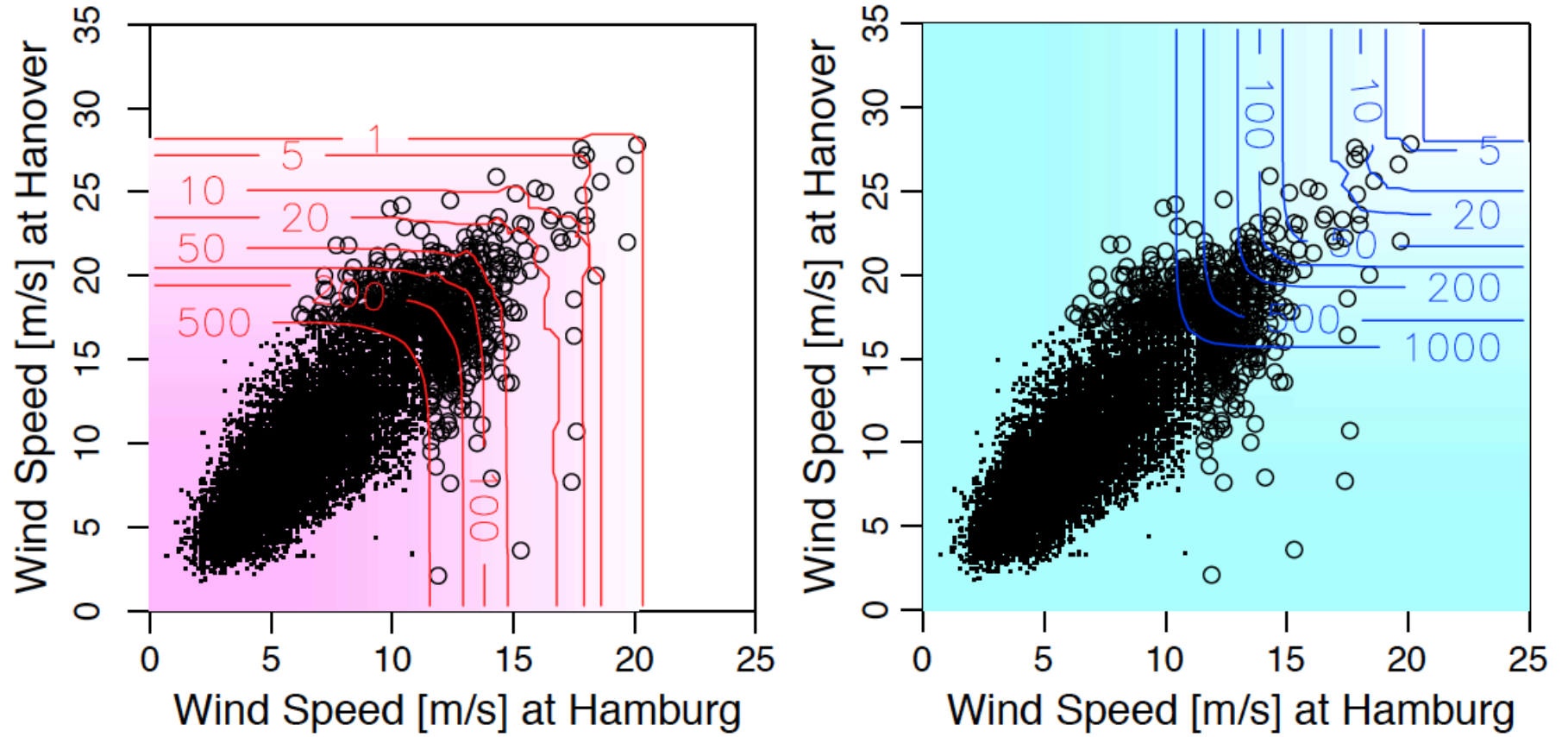
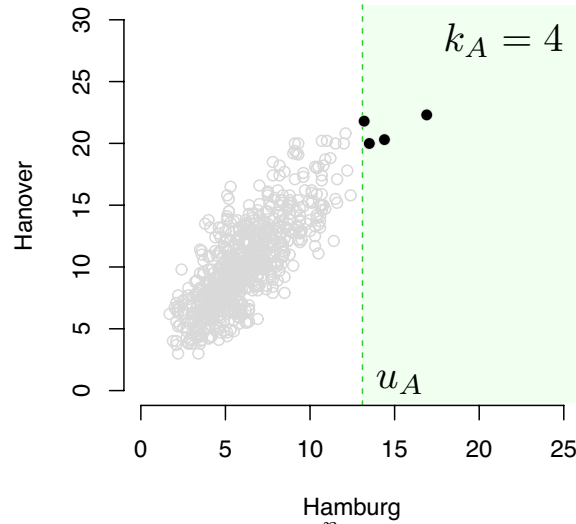
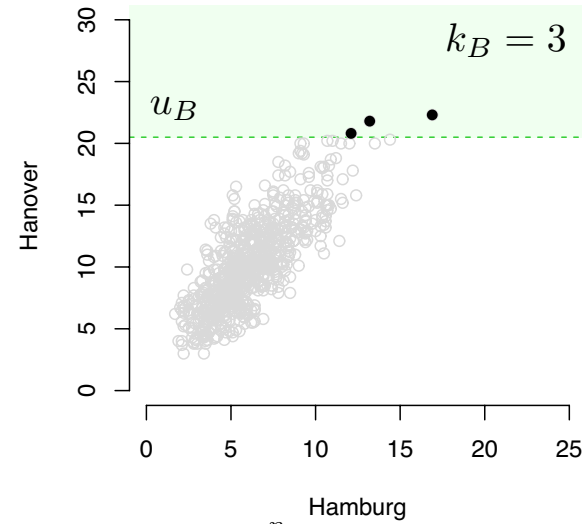


Fig.1 Joint occurrence numbers and the inclusive occurrence numbers against two components' thresholds (The data of small values are marked not by circles but by dots simply on account of reducing image size)

# Counting the excess numbers is another way of evaluating extremes, ...

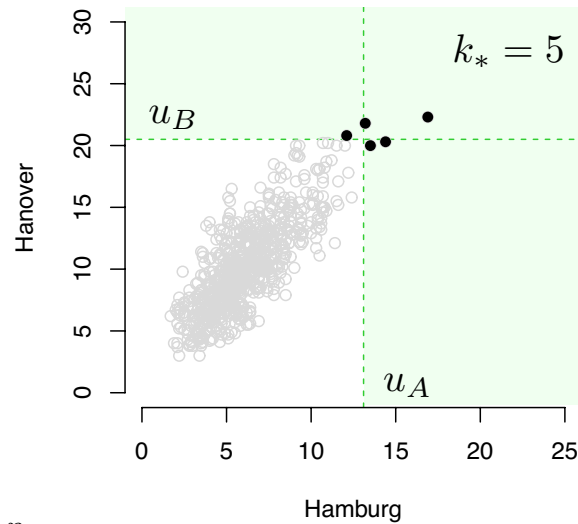


$$k_A(u_A) = \sum_{i=1}^n \mathbf{1}\{Y_A(i) > u_A\},$$



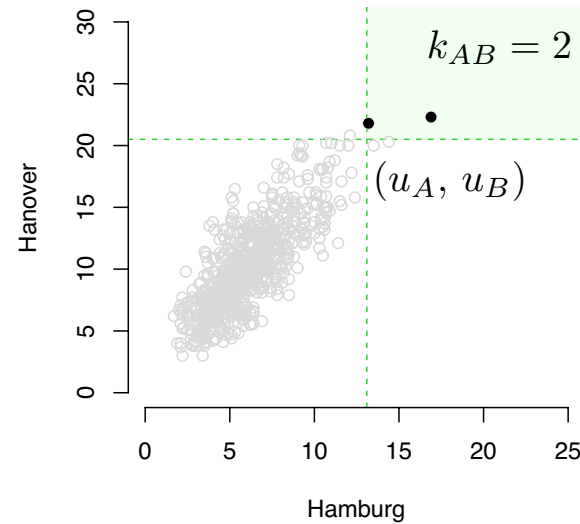
$$k_B(u_B) = \sum_{i=1}^n \mathbf{1}\{Y_B(i) > u_B\}$$

## Inclusive occurrence number



$$k_*(u_A, u_B) = \sum_{i=1}^n \mathbf{1}\{Y_A(i) > u_A\} \vee \mathbf{1}\{Y_B(i) > u_B\}$$

## Joint occurrence number



$$k_{AB}(u_A, u_B) = k_A(u_A) + k_B(u_B) - k_*(u_A, u_B)$$

The joint occurrence number  $k_{AB}$  is defined as the excess number against both thresholds  $(u_A, u_B)$ , whose contour lines are shown as making thresholds of each point in the left figure. The excess numbers are given as the actual ones in the observation time length (40 years). In order to extrapolate the occurrence number for the outside (white region in that figure), we use the occurrence rate in the mathematical function to fit to the observed data. However the mathematical theory cannot be build directly for the joint occurrence  $k_{AB}$ , and it can be based on the inclusive occurrence number  $k^*$  which is the excess number against at least either of thresholds of two components, as described in the mathematical terms:

$$k_*(u_A, u_B) = k_A(u_A) + k_B(u_B) - k_{AB}(u_A, u_B) = \sum_{i=1}^n \mathbf{1}\{Y_A(i) > u_A\} \vee \mathbf{1}\{Y_B(i) > u_B\} \quad (2)$$

where  $a \vee b = a$  for  $a \geq b$ , or  $a \vee b = b$  for  $a < b$ . The left figure of Fig.1 shows the contour lines of the inclusive occurrence numbers. One of the important keys to understand the occurrence of bivariate extremes is to know the theoretical background that these counting numbers are related to the bivariate Poisson distribution.

$$p(k_A, k_B) = e^{-\lambda_*(u_A, u_B)} \sum_{j=0}^{k_A \wedge k_B} \frac{\lambda_{AB}^j}{j!} \frac{\{\lambda_A(u_A) - \lambda_{AB}(u_A, u_B)\}^{k_A-j}}{(k_A - j)!} \frac{\{\lambda_B(u_B) - \lambda_{AB}(u_A, u_B)\}^{k_B-j}}{(k_B - j)!} \quad (3)$$

where  $a \wedge b = b$  for  $a \geq b$ , or  $a \wedge b = a$  for  $a < b$ . The mean occurrences  $\lambda_A, \lambda_B, \lambda_{AB}$  and  $\lambda^*$  are the expected values of the corresponding counting numbers  $k_A, k_B, k_{AB}$  and  $k^*$ . The case of no occurrence for both components  $k_A = 0$  and  $k_B = 0$  gives the cumulative distribution function of the bivariate component-wise maxima

$$F(x, y) = e^{-\lambda_*(x, y)} \quad (4)$$

which has a great history of many amounts of researches illustrated by the pioneering works by Sibuya (1960) and Pickands (1981), etc. One of the most notable findings based on the measure theory for the multivariate extreme value theory told us that the exponent of the cumulative distribution function  $F$  of component-wise maxima, equivalently that is the inclusive occurrence rate  $\lambda^*$ , is not given as an unique, nor several models, but infinite number of functions which are described in the general form

$$\lambda_*(x, y) = \int_0^1 \{\omega \lambda_A(x)\} \vee \{(1 - \omega) \lambda_B(y)\} dH(\omega) \quad (5)$$

by employing the so-called spectral function  $H$ , which is a kind of cumulative distribution so that the total amount is the number of dimension in general sense, that is,  $H(1) = 2$  in the bivariate case. Based on this fact, Beirlant et al.



For one-component, it will be easier to understand the relation between the Poisson distribution and the extreme variable.

The uni-variate Poisson distribution is described in terms of the mean rate as follows:

$$f(k) = \frac{\lambda_1^k}{k!} e^{-\lambda_1}$$

The case of no occurrence gives the cumulative distribution (= non-exceedance probability) function:

$$f(k=0) = e^{-\lambda_1} \rightarrow G_1(y) = e^{-\lambda_1} \big|_{\lambda_1 = \lambda_1(y)} = e^{-\lambda_1(y)}$$

where the rate function is set to  $\lambda_1(y) = \left(1 + \xi \frac{y - \mu_1}{\sigma_1}\right)^{-1/\xi}$

then Eq.(\*) corresponds to a GEV (Generalized Extreme Value) distribution.

$$G_1(y) = \exp \left\{ - \left(1 + \xi \frac{y - \mu_1}{\sigma_1}\right)^{-1/\xi} \right\}$$

Key 2': A Poisson distribution into an extreme value d.

\* Univariate case:

$$p(k_x = 0) = \frac{\{\lambda_1(x)\}^0}{0!} e^{-\lambda_1(x)} = \exp \left\{ - \left( 1 + \xi_x \frac{x - \mu_{x,1}}{\sigma_{x,1}} \right)^{-1/\xi_x} \right\} \\ = F_1(x)$$

No occurrence prob.

= cumulative prob. distribution of max.

\* Bivariate case:

$$p(k_{x,1} = 0, k_{y,1} = 0) = e^{-\underline{\lambda_{*,1}(x,y)}} = F_1(x, y)$$

Therefore the **inclusive occurrence rate** becomes  
Important in the theoretical treatment.

$$\lambda_{*,1}(x, y) = E(k_*) = E \sum_i 1 \{X_i > x\} \vee 1 \{Y_i > y\}$$

pseudo polar coordinates

$$x'_1 = rt$$

$$y'_1 = r(1 - t)$$

H is constrained only by:

$$\int_0^1 dH(t) = 2$$

$$\int_0^1 t dH(t) = \int_0^1 (1 - t) dH(t) = 1$$

And more, ...

$$= \int 1 \left\{ \frac{x'_1}{x_1} \vee \frac{y'_1}{y_1} > 1 \right\} dV(x'_1, y'_1)$$

$$= \int 1 \left\{ r > \frac{x_1}{t} \wedge \frac{y_1}{1-t} \right\} dV(r, t)$$

$$= \int_0^1 \int_{\frac{x_1}{t} \wedge \frac{y_1}{1-t}}^{\infty} \frac{dr dH(t)}{r^2}$$

$$= \int_0^1 \left( \frac{t}{x_1} \vee \frac{1-t}{y_1} \right) dH(t) \quad \text{Finally !}$$

$$= \int_0^1 \{t\lambda_1(x) \vee (1-t)\lambda_1(y)\} dH(t)$$

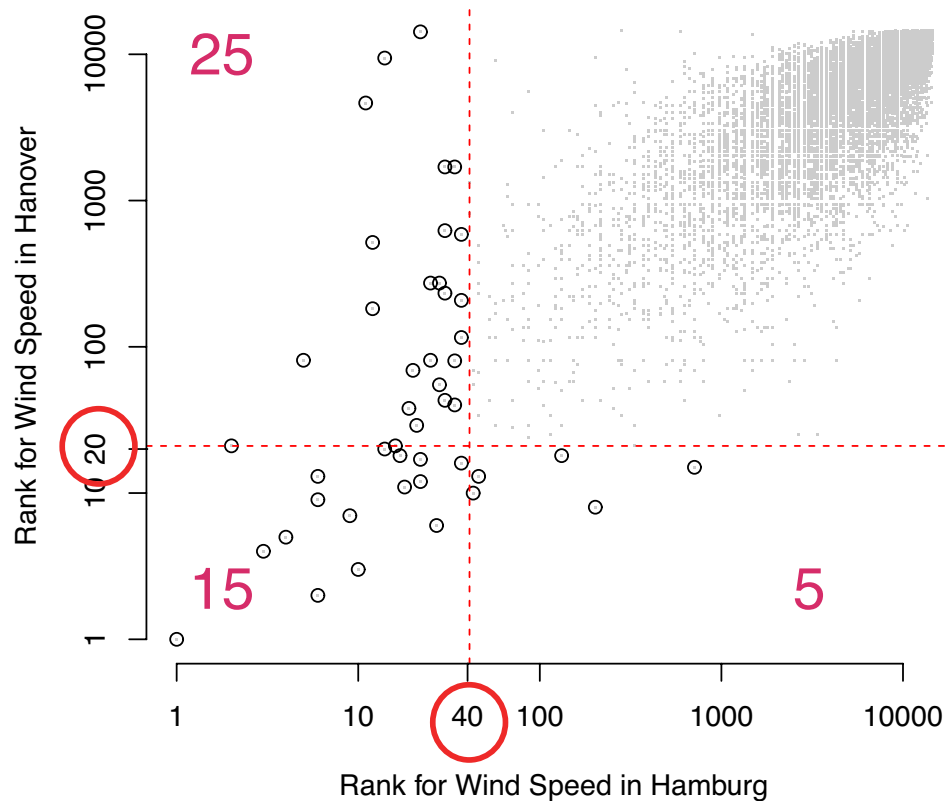
Pickands dependent function

$$A(\omega) = \frac{\lambda_{*,1}(x, y)}{\lambda_1(x) + \lambda_1(y)} = \int_0^1 \{t(1 - \omega) \vee (1 - t)\omega\} dH(t)$$

$$\omega = \frac{\lambda_1(y)}{\lambda_1(x) + \lambda_1(y)} = \frac{x_1}{x_1 + x_2}$$

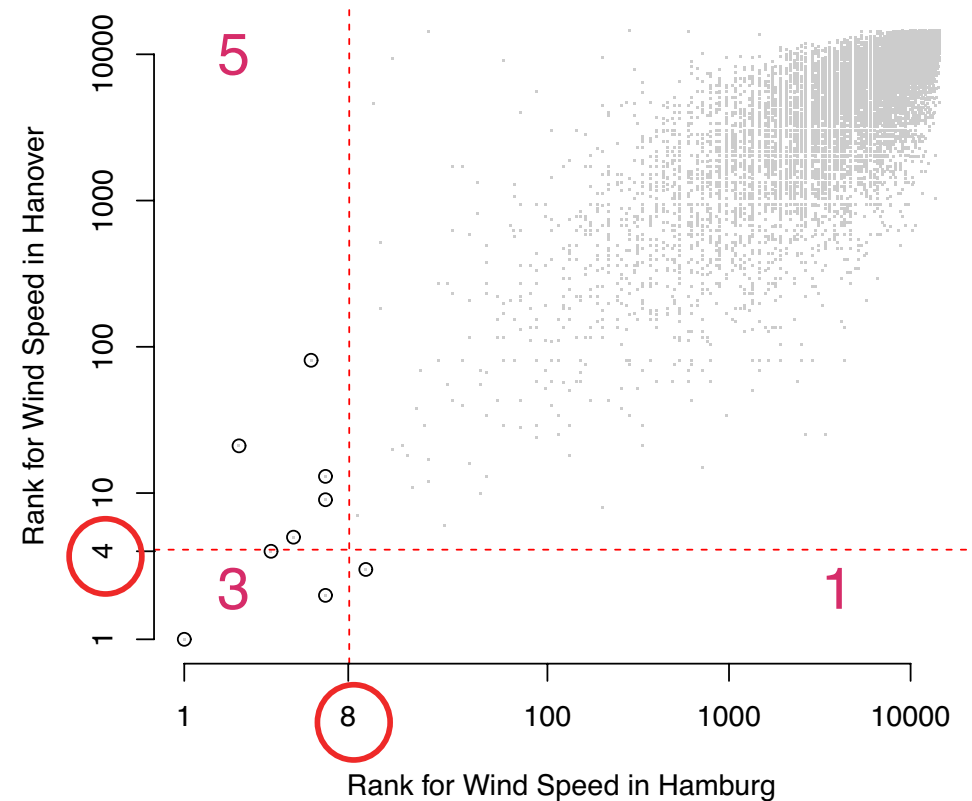


Essential for bivariate extremes: **Homogeneity** (of order - 1)  
 whose property shows the **proportionality & similarity** of the occurrence rate.  
 And it will be checked by using the sample data.



$$25 + 15 = 40$$

$$5 + 15 = 20$$



$$5 + 3 = 8$$

$$1 + 3 = 4$$

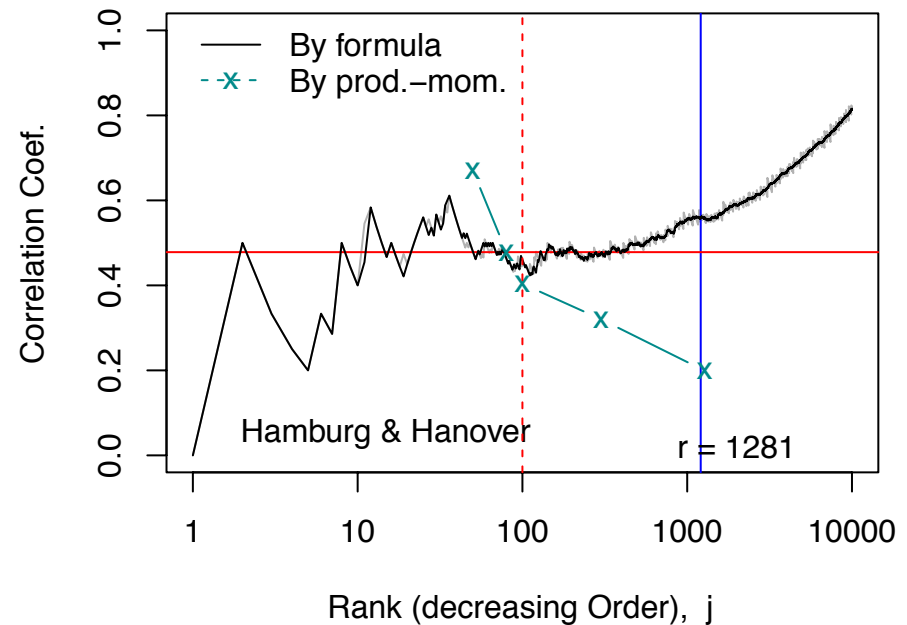
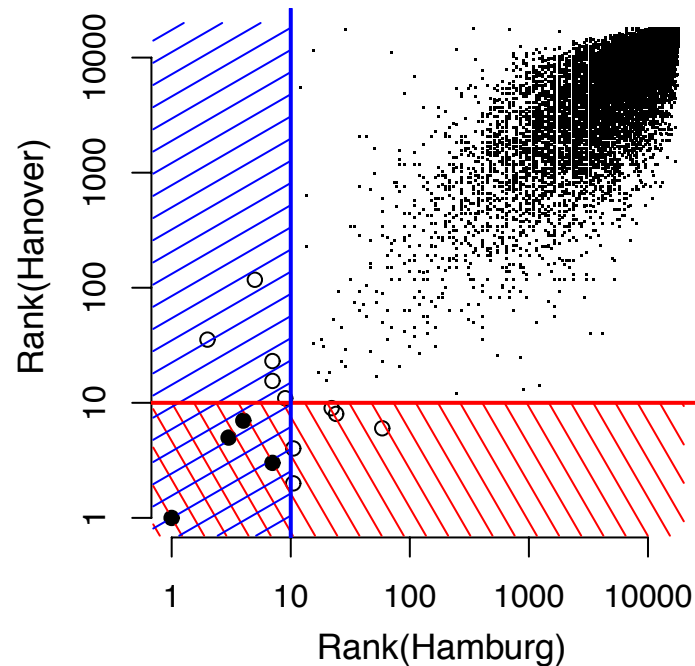
where we know ranks in decreasing order indicate the occurrence numbers.

Correlation coef. of occurrence numbers is given by  $\rho_{xy} = \frac{\lambda_{xy}}{\sqrt{\lambda_x \lambda_y}}$   
 which is based on the **bivariate Poisson distribution**, and it will be  
**estimated by sample**, as

$$\hat{\rho}_{xy} = \frac{k_{xy}}{j}$$

for the common number of rank  $j$ .  
 cf. c.c. by prod. mom. est.

$$\tilde{\rho}_{xy} = \frac{\sum (k_x - \bar{k}_x)(k_y - \bar{k}_y)}{\sqrt{\sum (k_x - \bar{k}_x)^2 \sum (k_y - \bar{k}_y)^2}}$$



## Contingency tables for excess & no excess

$u_x \setminus u_y$	Excess	No Excess	Total
Excess	20	25	45
No Excess	19	(667)	(686)
Total	39	(692)	(731)

Daily max.  
wind speeds  
for 2 years

$u_x \setminus u_y$	Excess	No Excess	Total
Excess	$k_{xy}$	$k_x - k_{xy}$	$k_x$
No Excess	$k_y - k_{xy}$	$(n - k_x - k_y + k_{xy})$	$(n - k_x)$
Total	$k_y$	$(n - k_y)$	$(n)$

### Perfect dependent

$u_x \setminus u_y$	Excess	No Excess	Total
Excess	39	6	45
No Excess	0	(686)	(686)
Total	39	(692)	(731)

$$k_* = k_x \vee k_y$$

### Independent

$u_x \setminus u_y$	Excess	No Excess	Total
Excess	0	45	45
No Excess	39	(647)	(686)
Total	39	(692)	(731)

$$k_* = k_x + k_y$$

$$\Leftrightarrow k_{xy} = 0$$

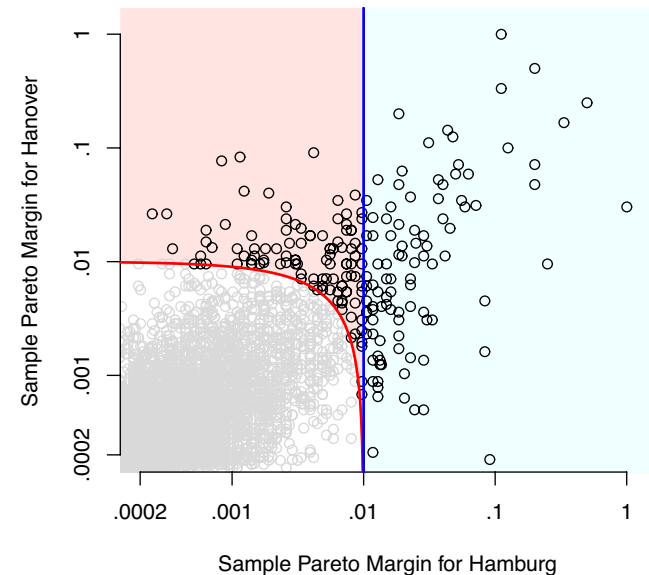
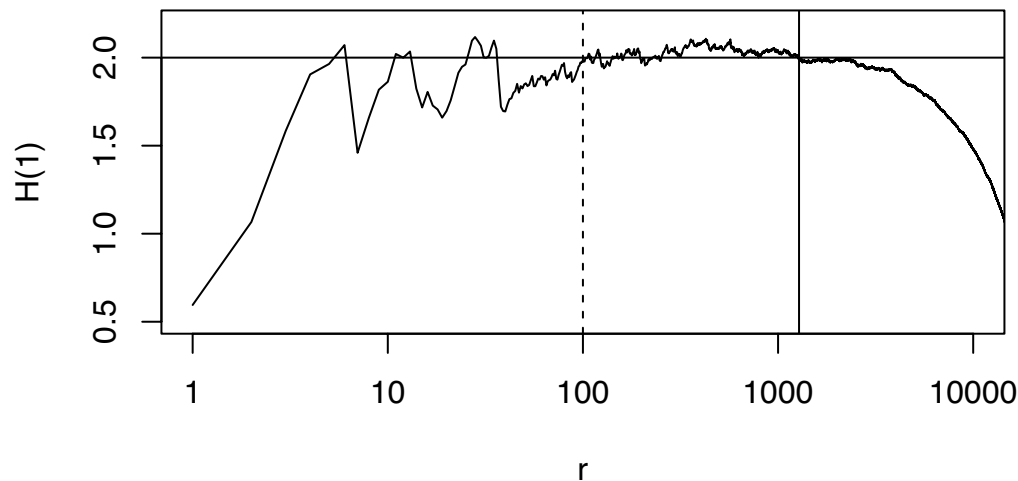


Conventional method uses the identity equation:  $H(1) = 2$

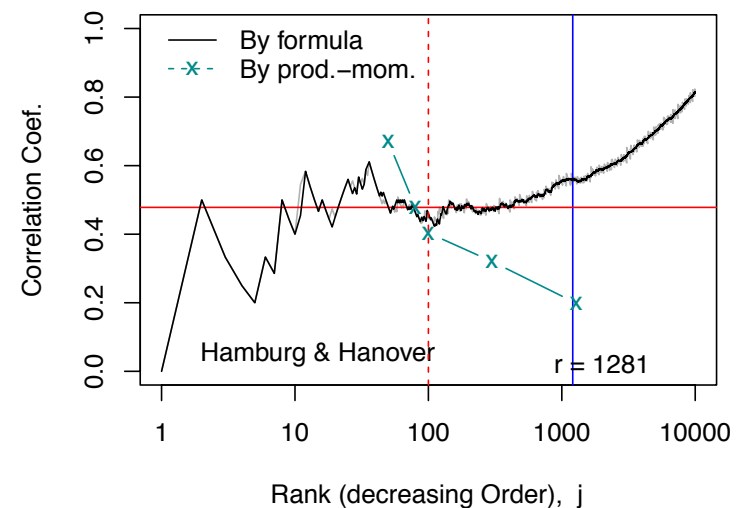
what this equation stands for?

-> The occurrence numbers are the same in the following **two** regions.

(The red line is a contourline of  $1/\text{rank}_A + 1/\text{rank}_B$ .)



However this method will be **overestimated**, as seen in this example where we can take  $r = 1281$ , while the C.C. is not stable. Actually the stable data is limited around 100.



$$\begin{aligned}
\lambda_*(x, y) &= E(k_*) = E \sum_i 1\{X_i > x\} \vee 1\{Y_i > y\} \\
&= \dots \text{ omitting the details of derivation } \dots \\
&= \int_0^1 \{\omega \lambda_A(x)\} \vee \{(1 - \omega) \lambda_B(y)\} dH(\omega)
\end{aligned}$$

The important thing is that demension reduction is possible by transforming the occurrence rate  $\lambda_*(x, y)$  into the Pickands dependence function  $A(t)$ . (Bivariate extreme distribution is so simple that there are included the wide range of the mathematical functions for the distributions.)

$$A(t) = \int_0^1 \{\omega(1 - t)\} \vee \{(1 - \omega)t\} dH(\omega)$$

where we define a transverse variabele

$$t = \frac{\lambda_B(y)}{\lambda_A(x) + \lambda_B(y)} = \frac{1/\lambda_A(y)}{1/\lambda_A(x) + 1/\lambda_B(y)}$$

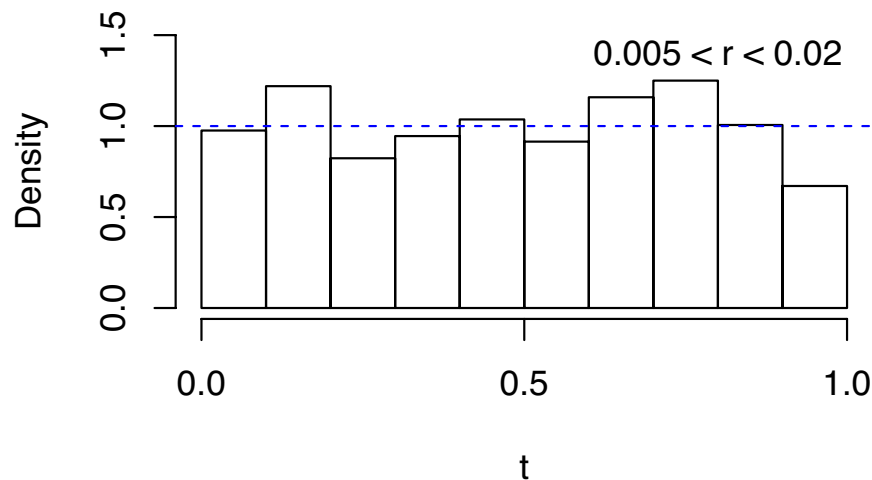
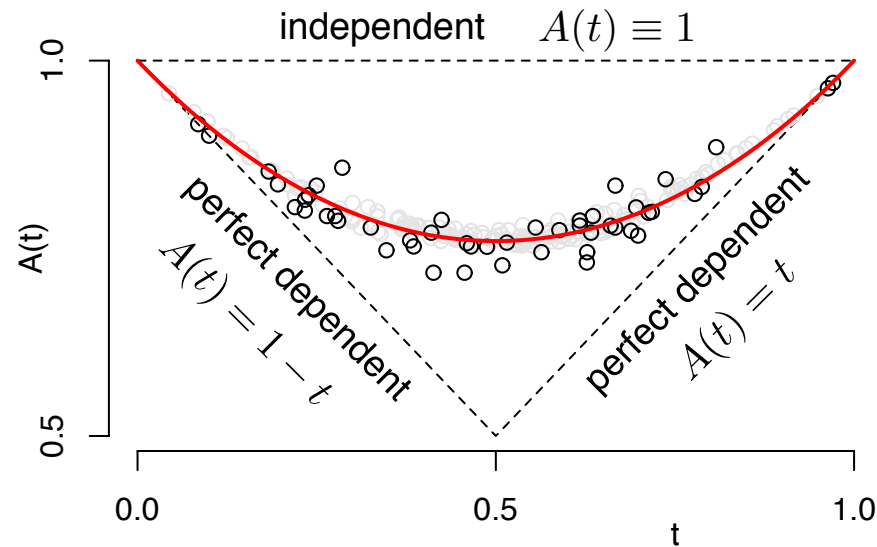
and the radius (lengthwise) variable

$$r = 1/\lambda_A(x) + 1/\lambda_B(y)$$

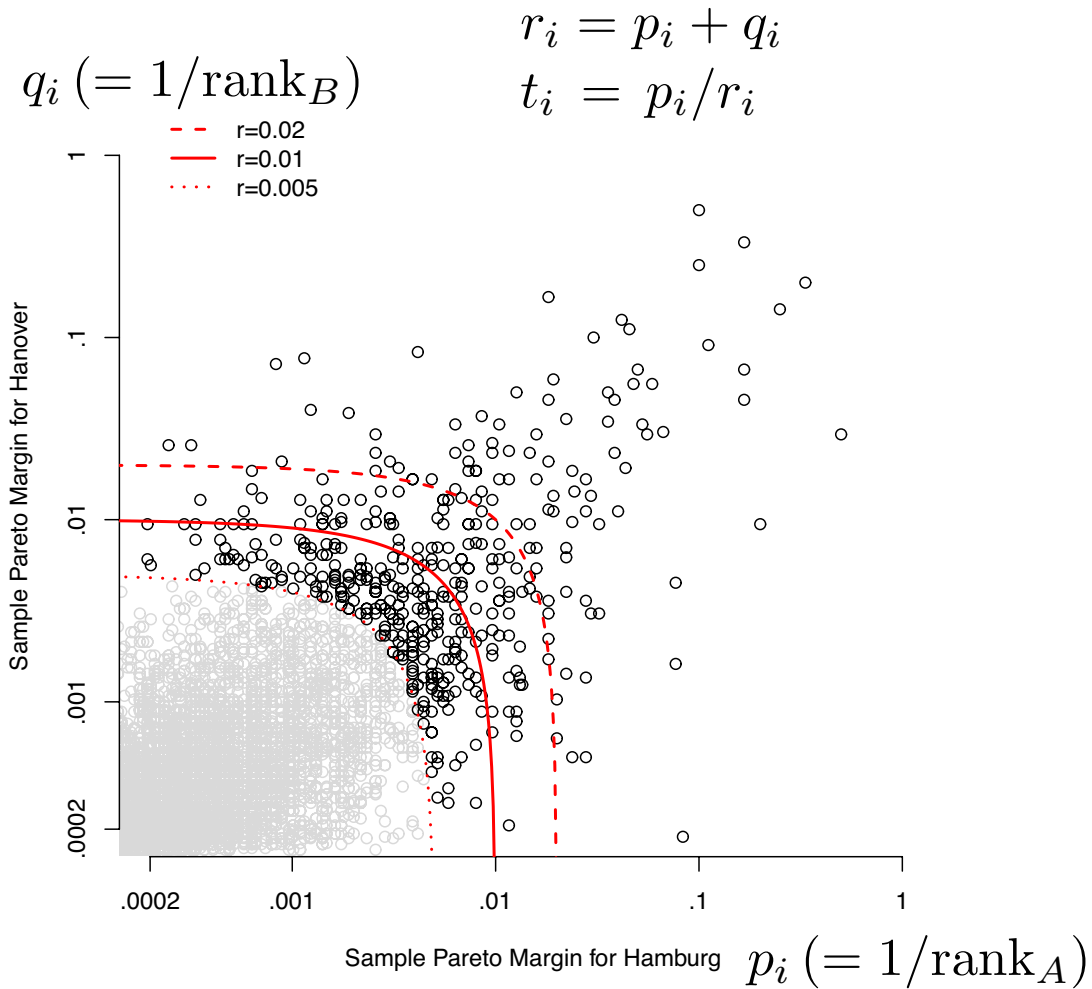
It is the pseudo polar coordinates.

Pickands dependence function shows well the dependency properties.

$$\tilde{A}_i = \frac{k_*}{\text{rank}_A + \text{rank}_B}$$

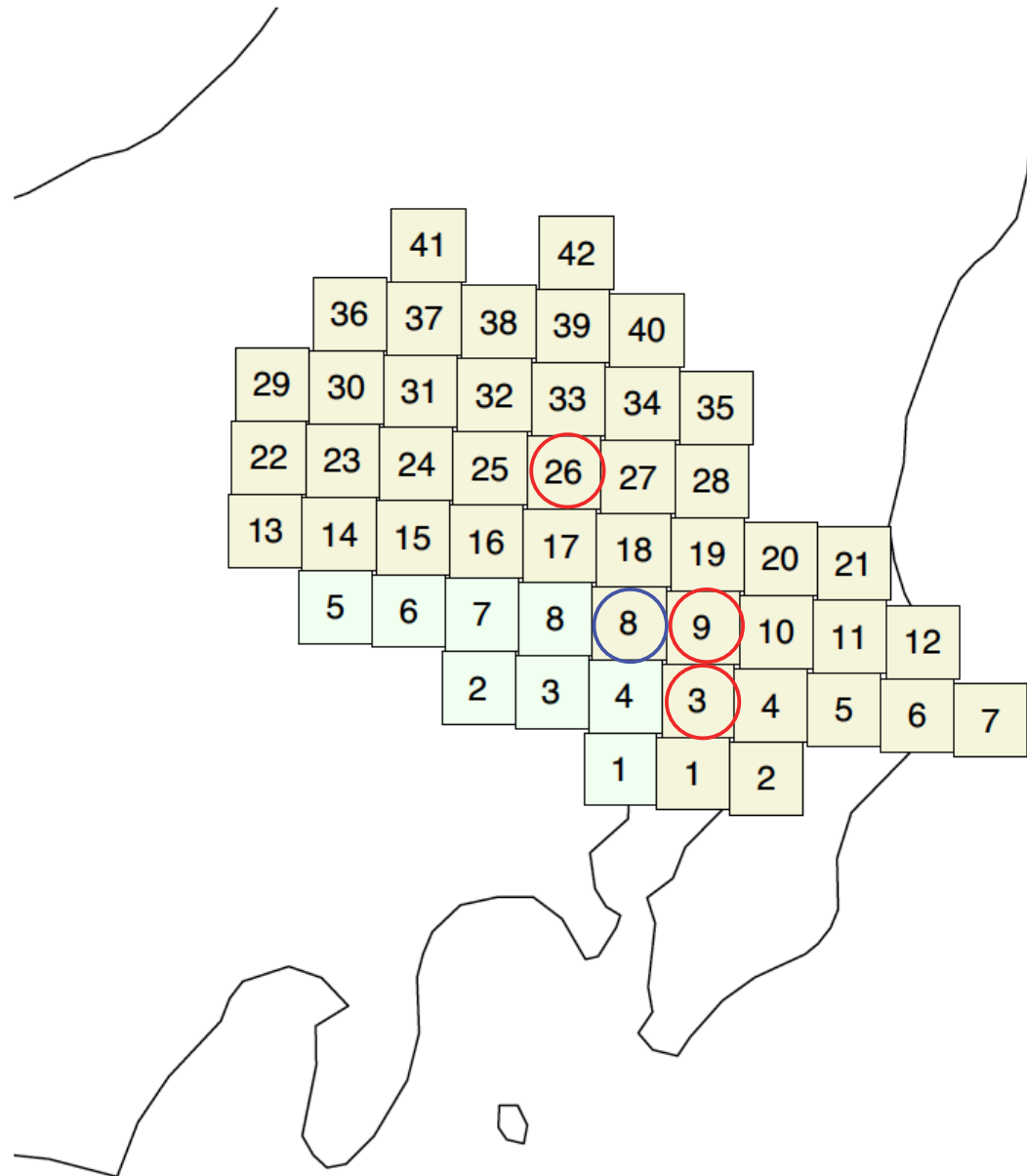


pseudo-polar coordinate

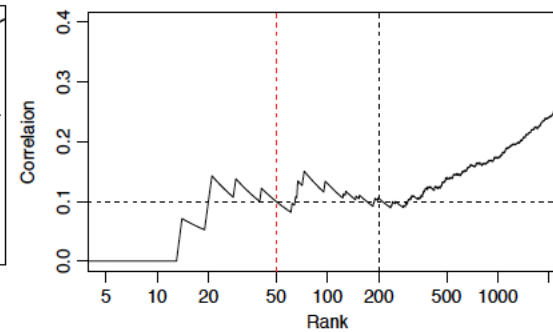
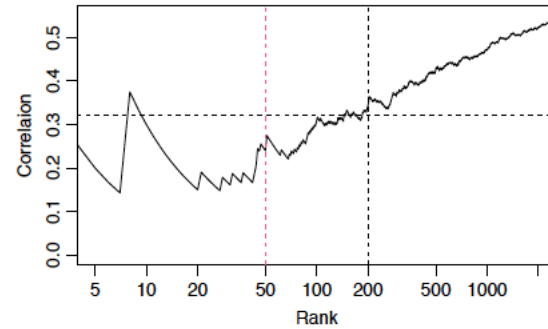
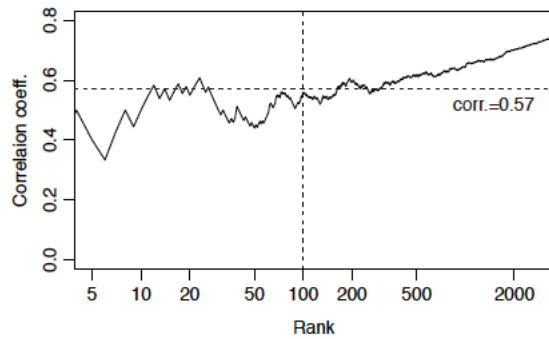


We analyze the spatial dependence of daily precipitations by using d4PDF.

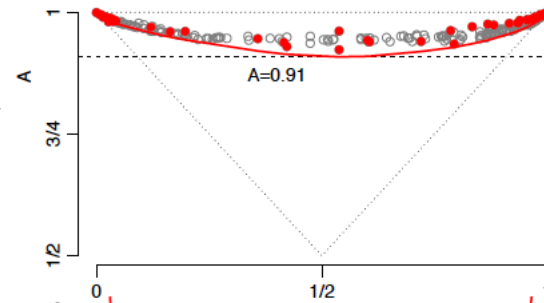
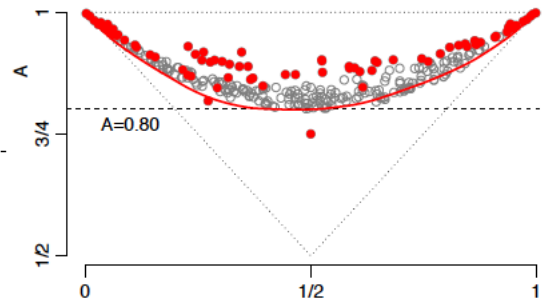
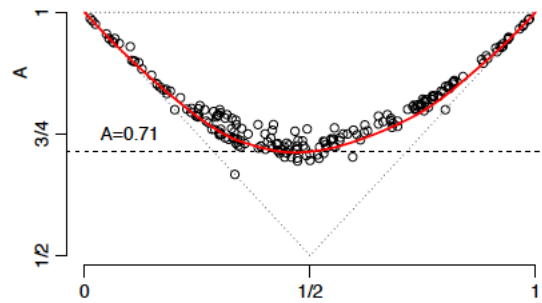
Map of cells in Tonegawa (in beige) and Arakawa (in light green) basins in Kanto plain is shown below.



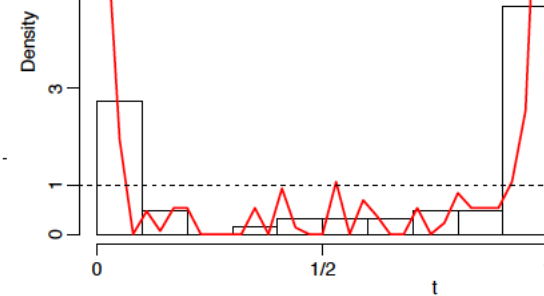
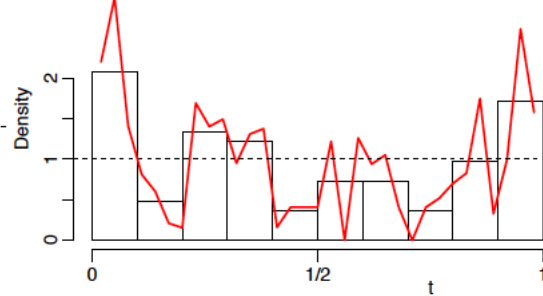
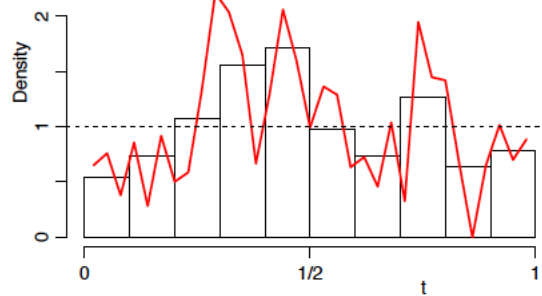




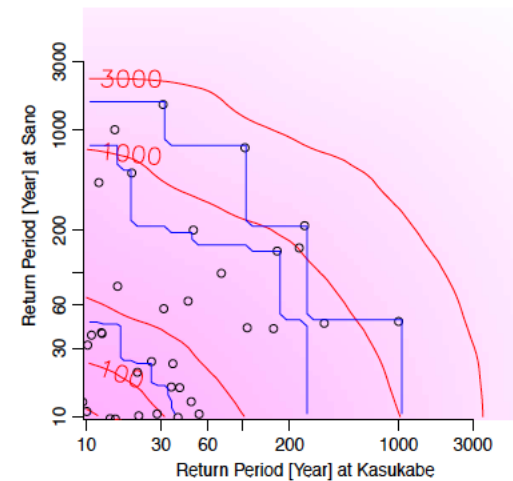
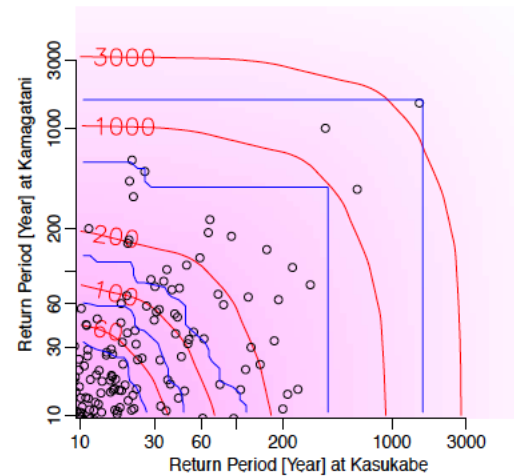
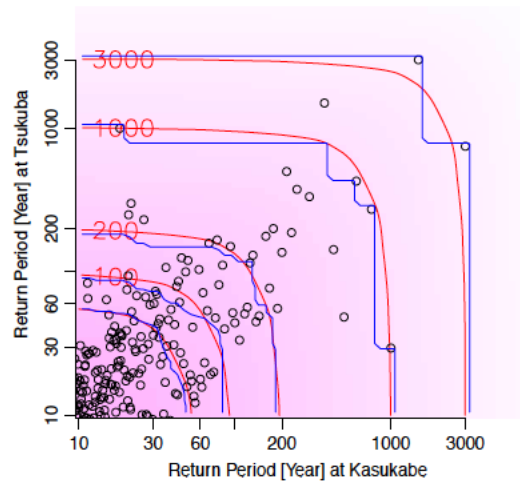
◁ Cor.  
Coef.



◁ Pickands  
Dependent  
Function



◁ Transverse  
Density



◁ Contours  
of Retrun  
Period of  
joint  
occurrences

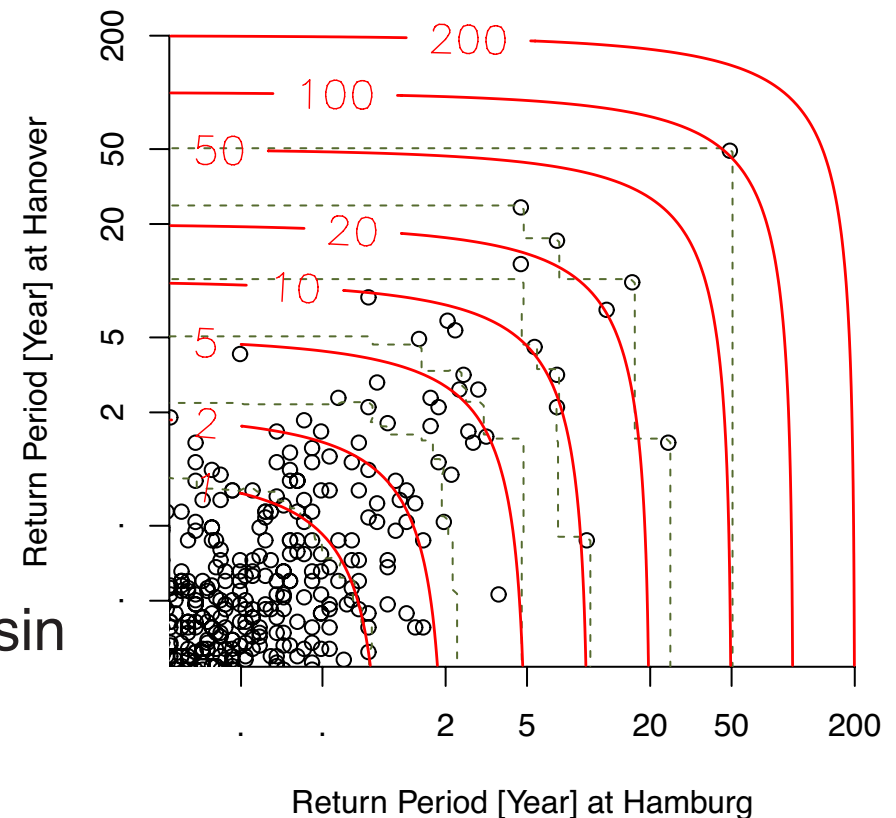
# Conclusions

What we show here today is actually **not new in extreme value theory**. But these facts have **not been well known** for hydrology and water-related engineering (Coastal and Hydraulic Eng.).

**Parametric approach** as well as **non-parametric approach** should be applied, because the wide range of parametric functions is possible to describe the joint (or inclusive) occurrence rate.

It is so important to examine the joint occurrence rates (and the return period) for the **accumulative risk**.

For the future works, the bivariate extreme analysis should be extended to the **spatial modeling** of the whole river basin and the comprehensive coastal zone.



# BIVARIATE EXTREME STATISTICS, I

By MASAAKI SIBUYA

(Received Jan. 20, 1960)

## 0. Introduction and Summary

The largest and the smallest value in a sample, and other statistics related to them are generally named extreme statistics. Their sampling distributions, especially the limit distributions, have been studied by many authors, and principal results are summarized in the recent Gumbel's book [1].

The author extends here the notion of extreme statistics into bivariate distributions and considers the joint distributions of maxima of components in sample vectors. This Part I treats asymptotic properties of the joint distributions.

In the univariate case the limit distributions of the sample maximum were limited to only three types. In the bivariate case, however, types of the limit joint distributions are various: Theorem 5 in Chapter 2 shows that infinitely many types of limit distributions may exist. For a wide class of distributions, two maxima are asymptotically independent or degenerate on a curve. Theorems 2 and 4 give the attraction domains for such limits. In bivariate normal case, two maxima are asymptotically independent unless the correlation coefficient is equal to one.

Throughout these arguments we remark only the dependence between marginal distributions, whose behaviours are well established. For this purpose a fundamental notion of "dependence function" is introduced and discussed in Section 1.

A practical application will be considered in the subsequent paper.